

COHERENT TIMING OF THE ACCRETING MILLISECOND PULSAR NGC 6440 X-2

PETER BULT¹, ALESSANDRO PATRUNO^{2,3}, AND MICHEL VAN DER KLIS¹*Draft Version October 22, 2015.*

ABSTRACT

We study the 205.9 Hz pulsations of the accreting millisecond X-ray pulsar NGC 6440 X-2 across all outbursts observed with the *Rossi X-ray Timing Explorer* over a period of 800 days. We find the pulsations are highly sinusoidal with a fundamental amplitude of 5% – 15% rms and a second harmonic that is only occasionally detected with amplitudes of $\lesssim 2\%$ rms. By connecting the orbital phase across multiple outbursts, we obtain an accurate orbital ephemeris for this source and constrain its 57 min orbital period to sub-ms precision. We do not detect an orbital period derivative to an upper limit of $|\dot{P}| \leq 8 \times 10^{-11} \text{ s s}^{-1}$. We investigate the possibility of coherently connecting the pulse phase across all observed outbursts, but find that due to the poorly constrained systematic uncertainties introduced by a flux-dependent bias in the pulse phase, multiple statistically acceptable phase-connected timing solutions exist.

Subject headings: pulsars: general – stars: neutron – X-rays: binaries – pulsars: individual (NGC 6440 X-2)

1. INTRODUCTION

Accreting Millisecond X-ray Pulsars (AMXPs) are rapidly rotating neutron stars in low-mass X-ray binaries. These systems show coherent X-ray pulsations that arise when the accretion flow is magnetically channeled to the stellar surface. These pulsations offer a physical tracer of the neutron star and the inner accretion flow toward it, as their frequency gives a direct measure of the neutron star rotation rate, and the shape of the pulse waveform carries information on the accretion geometry and compactness of the neutron star (Poutanen & Gierliński 2003; Leahy et al. 2008; Psaltis et al. 2014). Tracking the pulse arrival times allows to measure the evolution of the neutron star spin and the binary orbit, thus offering insight into accretion torque theory (Psaltis et al. 1999), alternative torque mechanisms (Bildsten 1998; Haskell & Patruno 2011) and the binary evolution of millisecond pulsars (Bildsten 2002; Nelson & Rappaport 2003; Patruno et al. 2012).

Among the currently known AMXPs (see Patruno & Watts 2012 for a review), the globular cluster source NGC 6440 X-2 is unique in its outburst behavior; it shows comparatively short, low luminosity outbursts, with peak X-ray luminosities of $L_X \lesssim 1.5 \times 10^{36} \text{ erg s}^{-1}$ and outburst durations of 2 – 5 days (Heinke et al. 2010). NGC 6440 X-2 was discovered with Chandra on July 28th, 2009 (Heinke et al. 2009) and seen in outburst again merely a month later with the *Rossi X-ray Timing Explorer* (*RXTE*), at which time the 205.9 Hz pulsations were discovered (Altamirano et al. 2009). The following two outbursts each occurred after a quiescent interval of about one month, establishing NGC 6440 X-2's recurrence time as the shortest of all AMXPs known to date. The coherent timing analysis of those first four outbursts

was reported by Altamirano et al. (2010b), who found pulsations in three outbursts at fractional amplitudes of $\sim 7\%$ for the fundamental component.

After the fourth outburst, on October 28th, 2009, no activity from NGC 6440 X-2 was observed until March, 2010, although outbursts may have been missed due to visibility constraints and activity from other X-ray sources the same field (Altamirano et al. 2010a). Subsequently, the source showed another three outbursts with a recurrence time of about 110 days, after which it remained undetected for nearly 300 days until the last outburst was observed with *RXTE* in November, 2011 (Patruno & D'Angelo 2013).

In this work we present the results of a coherent timing analysis of NGC 6440 X-2 over the course of its complete outburst history as observed with *RXTE*. In Section 2 we describe our data reduction and analysis method. In Section 3 we present our results as we discuss how the high precision orbital ephemeris and pulse frequency evolution of NGC 6440 X-2 was obtained. Next, in Section 4, we briefly summarize and discuss our results.

2. DATA REDUCTION

We analyze all pointed *RXTE* observations of NGC 6440 X-2 (Altamirano et al. 2009; Heinke et al. 2010; Patruno & D'Angelo 2013). We use the 16-s time-resolution Standard-2 data to construct 2–16 keV light curves, normalized to the count rate of the Crab ($\sim 2300 \text{ ct s}^{-1} \text{ PCU}^{-1}$; $\sim 2.8 \times 10^{-8} \text{ erg cm}^{-2} \text{ s}^{-1}$) and averaged per observation (see, e.g., van Straaten et al. 2003 for details). We find one type I X-ray burst at MJD 55359.5, which we exclude from our further analysis.

For the timing analysis we use all high time resolution ($\leq 122 \mu\text{s}$) SingleBit, Event and GoodXenon data. We correct the data to the Solar System barycenter using the FTOOL *fbary* based on the Chandra X-ray position of Heinke et al. (2010). This tool also applies the *RXTE* fine clock corrections, allowing for an absolute timing precision of $\sim 4 \mu\text{s}$ (Rots et al. 2004).

The observations are divided in $\sim 500 \text{ s}$ segments,

¹ Anton Pannekoek Institute, University of Amsterdam, Postbus 94249, 1090 GE Amsterdam, The Netherlands

² Leiden Observatory, Leiden University, Postbus 9513, 2300 RA Leiden, The Netherlands

³ ASTRON, the Netherlands Institute for Radio Astronomy, Postbus 2, 7900 AA, Dwingeloo, The Netherlands

TABLE 1
OUTBURSTS OF NGC 6440 X-2

ID	Date	T_{asc} (MJD)	ΔMJD (days)	ObsID	Exposure (s)	Pulse Amp. (% rms)
$\mathcal{O}2$	2009-07-28	55042.81		94044-04-01-00 ^a	1900	12.9 ± 4.1
$\mathcal{O}3$	2009-08-30	55073.03	30.3	94044-04-02-00 ^b	3200	9.0 ± 0.5
		94044-04-02-01	14000	5 ^c
$\mathcal{O}4$	2009-10-01	55106.01	32.9	94044-04-03-00	2200	11.4 ± 1.9
		94044-04-04-00	3400	16 ^c
$\mathcal{O}5$	2009-10-28	55132.90	27.0	94315-01-04-01	900	14.0 ± 1.8
		94315-01-04-02	900	10 ^c
$\mathcal{O}6$	2010-03-21	55276.62	143.3	94315-01-12-00	2000	12.4 ± 0.7
		94315-01-12-01	2700	13.2 ± 1.0
		94315-01-12-02	1900	12.9 ± 1.1
$\mathcal{O}7$	2010-06-12	55359.47	83.2	94315-01-14-00	9900	7.6 ± 0.4
$\mathcal{O}8$	2010-10-04	55473.85	114.4	94315-01-25-00	1200	5.3 ± 0.6
$\mathcal{O}9$	2011-01-23	55584.71	110.9	96326-01-02-00	2100	6.0 ± 0.6
$\mathcal{O}10$	2011-03-21	55641.02	56.3	96326-01-10-00	2000	12.7 ± 1.9
$\mathcal{O}11$	2011-11-06	55871.23	231.9	96326-01-35-00	1200	6.3 ± 1.1
	...	55872.83		96326-01-40-00	3300	11.5 ± 2.3
	...	55873.31		96326-01-40-01	2400	9.8 ± 2.9

NOTE. — Pulse amplitudes are that of the fundamental component and calculated per *RXTE* orbit (~ 3 ks intervals). ΔMJD gives the duration of the quiescent interval with respect to the last observed outburst. Reported ObsIDs refer to Event mode data unless otherwise specified.

^a GoodXenon

^b SingleBit

^c 95% c.l. upper limit

selecting only the events in the energy channels 5–37 ($\sim 2 - 16$ keV), which optimizes the pulse signal to noise ratio. We then compare the observed count rate with the background count rate estimated using the *FTOOL pbackest*, and reject all observations for which the expected amplitude of a 100% modulated source contribution cannot be detected above the noise amplitude expected from counting statistics.

The remaining observations are corrected for the orbital ephemeris, folded on the pulse period (see Section 3), and fit with a constant plus a sinusoid at the fundamental (ν) and second harmonic (2ν) pulse frequency. We consider a pulse harmonic to be significant if its amplitude exceeds a detection threshold, which we define as the noise amplitude for which there is only a small probability $1 - \mathcal{C}$ that among all observations one or more exceed it by chance, and given a χ^2 distribution with 2 degrees of freedom for the squared amplitude of the noise. For a confidence level of $\mathcal{C} = 99\%$ and 500 second segments we then find a $A/\sigma_A = 3.8$ detection threshold, where A is the pulse amplitude and σ_A its uncertainty. Once an episode of pulsations has been established we repeat the analysis for several different segment lengths (100 – 3000 s) to study the pulse properties on various timescales. Pulse amplitudes are reported in terms of fractional rms

$$r_i = \frac{1}{\sqrt{2}} \frac{A_i}{N_\gamma - B}, \quad (1)$$

where A_i is the measured sinusoidal amplitude of the i -th harmonic, N_γ the total number of counts in the segment and B the estimated background contribution (see, e.g. Patruno et al. 2010).

We model the measured pulse arrival times per outburst using a circular orbit and constant pulse frequency. As such our timing model consists of four parameters, namely the orbital period P_b , the projected semi-major axis $A_x \sin(i)$, the time of the ascending node T_{asc} , and the pulse frequency ν . Phase residuals are obtained by subtracting this timing model from the measured arrival

times and analysed to refine the timing model. The details of this analysis are presented in the following section.

3. RESULTS

Because of the short duration of its outbursts and its high recurrence rate, the coherent timing analysis of NGC 6440 X-2 requires careful consideration. In this section we describe our analysis of this source in detail. We start from a provisional timing solution based on the work of Altamirano et al. (2010b), and iteratively refine the timing model parameters until the final timing solution is obtained.

Initially we consider the outbursts of NGC 6440 X-2 separately (see Table 1 for details). We refer to i -th outburst as $\mathcal{O}i$, where we start counting outbursts from an archival *Swift* observation on the 4th of June, 2009 (MJD 54986), which is considered the earliest detection of this source (Heinke et al. 2010). For our preliminary timing solution we adopt the pulse frequency, projected semi-major axis and orbital period that Altamirano et al. (2010b) obtained for $\mathcal{O}3$. Because of the limited accuracy of their orbital period measurement ($P_b = 3438(33)$ s) we cannot reliably predict the time of ascending node for any of the other outbursts. Instead, for each outburst, we set this parameter by searching a grid of T_{asc} at a 5-second resolution and selecting the value that maximizes the pulse amplitude.

NGC 6440 X-2 has been reported to have shown nine outbursts observed with *RXTE* during the 800 day observational baseline (Patruno & D’Angelo 2013). We find pulsations during this baseline on ten occasions, adding one low-flux outburst ($\mathcal{O}10$) to the sample. Five of the observed outbursts reached a flux of ~ 9 mCrab, and the other five peaked at fluxes half that or lower (see Figure 1). The pulse profiles are highly sinusoidal, with typical fundamental pulse amplitudes of 5% – 15% rms and second harmonic amplitudes of $\sim 2\%$ detected for only three observations ($\mathcal{O}3$, $\mathcal{O}7$, $\mathcal{O}9$). We report the details of each outburst in Table 1.

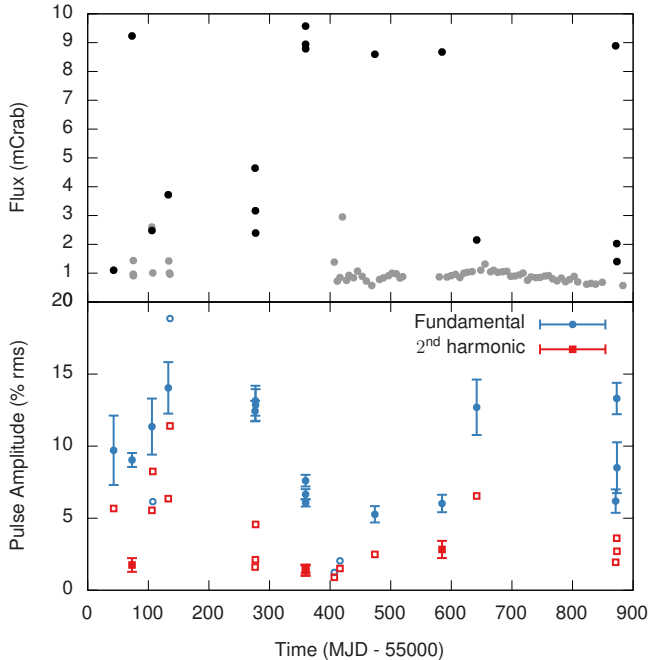


FIG. 1.— Top: light curve of NGC 6440 X-2 as observed with *RXTE*. Black points show observations with significantly detected pulsations, gray points show observations for which pulsations were not detected. Bottom: fundamental (blue circles) and second harmonic (red squares) fractional pulse amplitudes. Open symbols give 95% upper limits.

Although NGC 6440 X-2 has shown many outbursts, only a few observations offer sufficient quality to place useful constraints on the timing model parameters. Many of the observations have a low signal to noise ratio due to the low count rate of the source. Additionally, most outbursts are observed only for a single exposure of less than 3 ks, which is shorter than the orbital period of the binary. So, even if the phase could be measured on a sufficiently short timescale to allow for a fit to our 4-parameter timing model, the short exposures introduce strong correlations between ν , T_{asc} and P_b and hence cause a large uncertainty on all parameters.

For three outbursts of NGC 6440 X-2 the data is of sufficient quality to constrain the timing model. These are *O3*, *O6* and *O7*. The latter two are of particular use, as they consist of several consecutive exposures with separations of less than half a day. For these outbursts the data spans much more than a single orbital period, which breaks the correlation between the timing model parameters. We give the timing solutions for these outbursts in Table 2. While *O11* also consists of multiple exposures, we note that those observations are each about a day apart, and that, within the accuracy of the frequency measurement, the pulse phase cannot be uniquely propagated across that separation.

3.1. Orbital evolution

To refine the orbital period estimate, we consider the T_{asc} values measured locally for *O3*, *O6* and *O7* and perform a phase-coherent analysis of the orbital evolution. Using the timing solution of *O6* we predict the T_{asc} at the time of *O7* to obtain a difference between the predicted and locally measured T_{asc} of $\Delta T = 0.002(8)$ days.

Since the predicted T_{asc} and the local measurement are consistent, and the uncertainty is smaller than half the orbital period to within a 95% confidence level, we can coherently connect the orbital phase between these outbursts. Setting the estimated number of cycles between these outbursts, $N = (T_{\text{asc},7} - T_{\text{asc},6})/P_b$, to its nearest integer, then gives an accurate measurement of the orbital period of $P_b = 3457.892(2)$ s.

Using the phase-connected orbital period estimate we can describe all outbursts with a single orbital model. We therefore perform a joint-fit to the data using a timing model in which the orbital parameters are coupled, but the frequency is left free per outburst. This approach gives high accuracy measurements of the orbital parameters, which are presented in Table 3.

3.2. Spin frequency analysis

Because in a joint-fit approach the orbital parameters are fit to all data, and only the frequency is measured locally per outburst, the correlation between the orbit and spin parameters that occurs for short observations is no longer an issue. This method therefore allows the frequency to be measured in additional outbursts. The frequency measurements, shown in Table 3, are consistent within their respective uncertainties, and place a 95% confidence level upper limit on the frequency derivative of $|\dot{\nu}| \lesssim 5 \times 10^{-13} \text{ Hz s}^{-1}$.

As was done for the orbital phase, we may also attempt to connect the pulse phase between outbursts. To do this we construct a single pulse profile using all data of an outburst, from which we measure an averaged pulse arrival time. Starting from *O6*, which gives the most accurate frequency measurement, we then propagate the timing model to predict the pulse arrival time for the other outbursts. In this analysis, however, there are additional effects that contribute to the predicted phase or its uncertainty, which need to be accounted for.

The pulsations may show a frequency derivative that contributes to the phase difference between two outbursts. To be conservative we need to allow for the largest plausible frequency derivative, so while other AMXPs with a measured long term frequency evolution appear to be consistent with spin-down due to magnetic dipole braking, we note that we cannot assume this is also the case for NGC 6440 X-2; other torquing mechanisms may be present that produce a larger change of spin frequency (e.g. D’Angelo & Spruit 2012; Mahmoodifar & Strohmayer 2013). Typically torquing mechanisms are comparable or weaker than the accretion process, so we estimate the largest plausible (absolute) spin derivative from standard accretion theory (Patruno & Watts 2012)

$$\begin{aligned} \dot{\nu} \simeq & 4.2 \times 10^{-14} \gamma_B^{1/2} \\ & \times \left(\frac{\dot{M}}{2 \times 10^{-10} M_\odot \text{ yr}^{-1}} \right)^{6/7} \left(\frac{B}{10^8 \text{ G}} \right)^{2/7} \\ & \times \left(\frac{M}{1.4 M_\odot} \right)^{3/7} \left(\frac{R}{10 \text{ km}} \right)^{6/7} \text{ Hz s}^{-1} \end{aligned} \quad (2)$$

where $\gamma_B \simeq 0.3 - 1$ parameterizes the uncertainty in the angular momentum at the inner edge of the accretion disk (Psaltis et al. 1999), \dot{M} gives the mass accretion

TABLE 2
PER-OUTBURST TIMING SOLUTIONS

ID	ν (Hz)	$A_x \sin(i)$ (lt-ms)	P_b (s)	T_{asc} (MJD)	χ^2/dof
$\mathcal{O}3$	205.89217(14)	6.2(6)	3421(156)	55073.035(3)	3/5
$\mathcal{O}6$	205.8921768(2)	6.05(4)	3458.0(3)	55276.62545(3)	7/8
$\mathcal{O}7$	205.8921759(7)	6.14(2)	3458(1)	55359.51080(3)	14/24

TABLE 3
JOINT-FIT TIMING SOLUTION

Parameter	Value	Statistical uncertainty	Systematic uncertainty
P_b (s)	3457.8929	7×10^{-4}	
$ \dot{P}_b $ (s s^{-1})	$\leq 8 \times 10^{-11}$		
$A_x \sin(i)$ (lt-ms)	6.14	0.01	
T_{asc} (MJD)	55318.04809	2×10^{-5}	
ν_3 (Hz)	205.892177	3×10^{-6}	
ν_6 (Hz)	205.89217619	1.1×10^{-7}	2×10^{-6}
ν_7 (Hz)	205.8921758	7×10^{-7}	7×10^{-6}
ν_9 (Hz)	205.892185	1.7×10^{-5}	
ν_{10} (Hz)	205.89208	3×10^{-5}	
ν_{11a} (Hz)	205.89212	4×10^{-5}	
ν_{11b} (Hz)	205.89221	2×10^{-5}	
$ \dot{\nu} $ (Hz s^{-1})	$\leq 5 \times 10^{-13}$		

NOTE. — Joint-fit timing solution with coupled orbital parameters ($\chi^2/\text{dof} = 41/59$). ν_i gives the frequency of the i -th outburst, with ν_{11a} referring to the first observation of $\mathcal{O}11$ and ν_{11b} to the second (also see Table 1).

rate and M , R and B give the mass, radius and magnetic field strength of the neutron star, respectively. Assuming the pulse frequency derivative is of this order, it can cause a phase offset of ~ 1 cycle over the 80 day interval between $\mathcal{O}6$ and $\mathcal{O}7$, and so the possibility of a frequency derivative needs to be accounted for. As the frequency derivative is the second unknown contributing to the phase (the frequency being the first unknown) we need to consider the phase prediction for two outbursts to determine both parameters.

The phase residuals of the individual outbursts are subject to systematic uncertainties. As demonstrated by Patruno et al. (2009), the pulse phase shows a correlation with X-ray flux in most AMXPs. This correlation can be understood as the instantaneous accretion rate causing an offset in the hotspot position and thus a bias in the phase residual. If the flux changes linearly in time, it introduces a linear trend in the phase residuals that the standard rms-minimization method corrects for by adjusting the pulse frequency. This effect is particularly relevant for $\mathcal{O}6$ and $\mathcal{O}7$, which both show a decay in flux. However, because that flux decay is nearly linear as well we cannot constrain the potential effect of a phase-flux relation from the data of NGC 6440 X-2 alone. A strong correlation between phase and flux may well be present, but because it is completely degenerate with the pulse frequency in the timing model the phase bias cannot be distinguished from phase evolution intrinsic to the pulsar. To still obtain an approximate estimate for the size of this uncertainty we consider that for most AMXPs the phase bias due to the flux is much less than one cycle (Patruno et al. 2009) and adopt a maximum phase

offset of $\delta\phi = 0.15$ cycles. The systematic uncertainty in frequency is then given as $\sigma_\nu = \delta\phi/\delta t$, where δt is the timespan of the considered outburst sampled by observations.

Due to the phase-flux relation the pulse phase measured for an outburst consists of the underlying spin phase and the flux-induced bias. The phase propagation based on the timing model, however, only applies to the part due to the neutron star spin, and not the bias. If the phase-flux relation is indeed introduced by a geometrical effect such as a drifting hotspot position, then we might expect that when averaging over an entire outburst, the bias will average to a mean value determined by the system accretion geometry which is the same for all outbursts. In other words; if the outburst is sufficiently well sampled, then we may be able to calibrate the flux-induced phase bias, such that we can calculate a reference phase that is stable between outbursts. For NGC 6440 X-2, however, the observational sampling of the outbursts is very poor, and consequently the measured pulse phase may be offset from the outburst-long average. Additionally, because other AMXPs, most notably SAX J1808.4–3658, have been observed to show different phase-flux relations for different outbursts (Patruno et al. 2009), the size and direction of the bias are essentially unknown and cannot be trivially corrected for by considering the flux difference between outbursts. As such, the flux-induced bias on the typical pulse phase of an outburst has considerable uncertainty. To get at least a rough estimate of this uncertainty we adopt the same $\delta\phi = 0.15$ cycles noted above. For $\mathcal{O}6$ this uncertainty is roughly 10 times larger than the statistical uncertainty on the averaged pulse arrival time.

Taking the noted considerations into account we can propagate the pulse phase from $\mathcal{O}6$ to $\mathcal{O}7$. We then find an uncertainty on the residual phase of $\sigma_\phi = 14.4$. The number of trials that we need to consider is then calculated as

$$n = 2(z\sigma_\phi + \varphi_\nu) + 1, \quad (3)$$

where z gives the significance interval for the usual two-sided confidence level $\mathcal{C} = \text{erf}(z/\sqrt{2})$, $\varphi_\nu = 1$ gives the phase offset introduced by frequency derivative as estimated above, the factor two accounts for the fact that the phase offset can be positive and negative, and the added one accounts for the central trial that has a phase offset of less than half a cycle. We then find that for a 95% confidence level, we need to consider 59 possible ways to connect the phases between these outbursts. Similarly we propagate the pulse phase from $\mathcal{O}6$ to $\mathcal{O}5$ to find an uncertainty of $\sigma_\phi = 24.8$, implying we need to consider 100 possible ways to connect those phase measurements. Hence, there are 5900 combinations of ν and $\dot{\nu}$ that connect the phases of the three considered outbursts. To

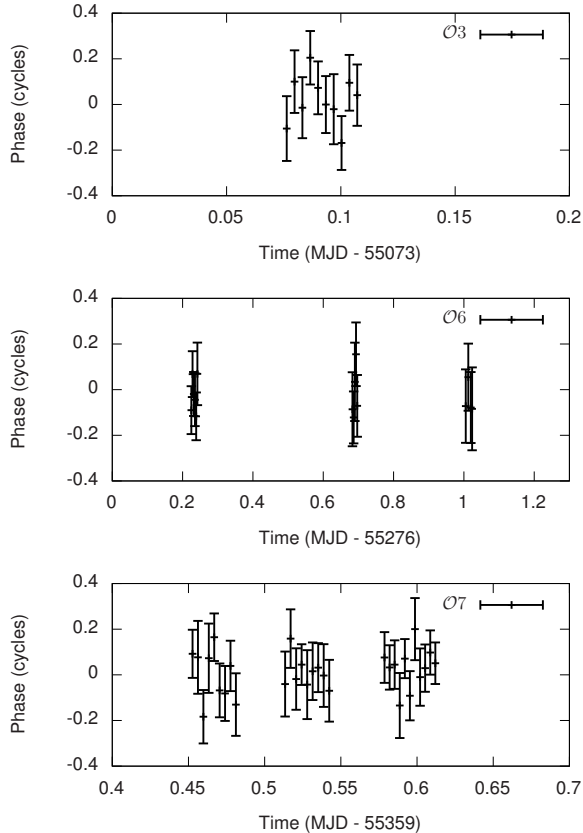


FIG. 2.— Phase residuals of the main outbursts for the phase connected timing solution assuming the the flux-induced phase bias is zero.

test these possible solutions we can propagate each trial solution to the other outbursts and calculate the χ^2 of the phase residuals to see which of them are statistically acceptable. However, due to the large phase uncertainty introduced by the phase bias we find that even for the trial solution that phase connects two outbursts the accumulated error on phase residuals at the time of the other outbursts is larger than 0.5 cycles even for the closest outburst. As such we cannot test the different trial solutions and must conclude that all 5900 considered options are statistically acceptable.

It is clear that the systematic uncertainty due to the phase-flux relation plays an important role, and that in the case of NGC 6440 X-2, it becomes prohibitive in the analysis of the long term spin evolution. Future observations may be able to establish the phase-flux relation in this source, allowing the size of the flux dependent phase bias to be calibrated per outbursts, thereby reducing the systematic uncertainties or potentially eliminating them altogether. To investigate whether a coherent pulse phase connection would then be feasible, we consider the scenario that the phase bias is zero in NGC 6440 X-2. Then, by accounting only for the statistical uncertainty on the frequency measurements, the number of trials we need to consider drops drastically from 100×59 to $8 \times 6 = 48$. Additionally, without the phase uncertainty due the flux, the error on the residual phases accumulates much slower, such that the trial timing solutions can be coherently extrapolated to O2 and O10.

Comparing each of the 48 solutions to the outbursts O2 through O10, we find that there is only one combination of ν and $\dot{\nu}$ that provides an statistically acceptable fit ($\chi^2/\text{dof} = 66/70$). Optimizing this solution by also re-fitting the orbital parameters and allowing for a second derivative on the pulse frequency, we find a pulse phase coherent timing solution that describes all data (including O11). We then have $\nu = 205.8921762261(3)$ Hz with $\dot{\nu} = 1.179(3) \times 10^{-14}$ Hz s $^{-1}$ and a second pulse frequency derivative of $\ddot{\nu} = -3.7(1) \times 10^{-23}$ Hz s $^{-2}$ (see Figure 2 for the phase residuals).

We stress that this result does not mean that the quoted solution necessarily gives the only correct description of this system. What it shows is that if the flux-induced phase bias can be calibrated, the correct phase coherent solution can be found. The solution mentioned above then gives the timing solution if the phase bias can be shown to be zero for this source.

4. DISCUSSION

We analysed the coherent pulsations of the accreting millisecond pulsar NGC 6440 X-2 for all outbursts observed with *RXTE*. We find that in the ten observed outbursts, the fundamental pulse amplitude varies from 5 to 15% rms, whereas the the second harmonic, if detected, has an amplitude of $\lesssim 2\%$ rms.

We have improved the orbital and spin parameter measurements of NGC 6440 X-2. Within the uncertainty of our measurements we find no evidence of a spin derivative to an upper limit of 5×10^{-13} Hz s $^{-1}$. This limit on the spin frequency derivative is larger than the expected spin-up or spin-down effects in AMXPs (see, e.g. Patruno & Watts 2012), and therefore does not constrain the neutron star spin evolution.

Through the coherent connection of the orbital phase, we measured the orbital period to high accuracy, but found no evidence of an orbital period derivative. These measurements are in line with expectations from binary evolution. As NGC 6440 X-2 is in an ultra-compact binary with a white dwarf companion star (Altamirano et al. 2010b), its orbital evolution is expected to be dominated by the loss of orbital angular momentum through the emission of gravitational waves (Kraft et al. 1962), with the evolution proceeding on a timescale of (Paczynski 1967)

$$T_{\text{GW}} = 50 \frac{(M + M_C)^{1/3}}{MM_C} P_b^{8/3} \text{ Gyr}, \quad (4)$$

where M the neutron star mass, $M_C \simeq 0.0076M_\odot$ the companion star mass and P_b is expressed in days. Assuming a canonical $1.4M_\odot$ neutron star we find a timescale of 1.4 Gyr, which implies an orbital derivate of $\dot{P} \sim 8 \times 10^{-14}$ s s $^{-1}$, much smaller than the upper limit we find in this work.

The short recurrence time of NGC 6440 X-2 hints at the possibility that like the orbital phase, the pulse phase may also be coherently connected across outbursts. Such a coherent phase connection would allow the spin frequency evolution of this source to be measured to high accuracy. We investigated the possibility of such a pulse phase connection, but could not find a unique timing solution. The flux induced phase bias known to exist in most AMXPs introduces systematic uncertainties in both

the frequency and phase measurements, which need to be taken into account. Unfortunately, due to the sparse observational sampling of NGC 6440 X-2's outbursts, the phase bias is degenerate with the pulse frequency parameter in the timing model. Consequently the presence and size of this phase bias could not be constrained.

Although we could not exclude the presence of a flux induced phase bias, we did attempt to phase connect the pulsations under the assumption that this effect does not occur for NGC 6440 X-2. We then find that a phase connection is possible and obtain a timing solution for a long term *spin-up* of the pulsar. Assuming typical outbursts last for about four days, the average duty cycle of NGC 6440 X-2 is about 5%, although we note this number may be slightly larger, as we may not have observed all outbursts. For this duty cycle the accretion spin-up during outburst would have to be about $2.4 \times 10^{-13} \text{ Hz s}^{-1}$. Based on accretion theory (eq. 2) such a large spin-up might be possible, but requires significant fine-tuning of the neutron star parameters (large neutron star mass and magnetic field strength). So, while this long term

spin-up is possible, it seems to us that it is more likely that it indicates the underlying assumption of zero phase bias does not hold and flux induced phase uncertainties indeed affect the observations of this AMXP.

Our analysis highlights the important role played by the systematic effects in pulse phase due to the X-ray flux when considering coherent timing of different outbursts. This applies not just to NGC 6440 X-2, but to any accreting millisecond pulsar.

We suggest that if future observations provide a better sampling of NGC 6440 X-2's outbursts and are able to constrain the size of the phase bias a coherent phase connection may be possible, warranting a closer investigation of this interaction between pulse phase and instantaneous X-ray flux and the mechanism by which it arises.

PB and MvdK acknowledge support from the Netherlands Organisation for Scientific Research (NWO). AP is supported by a NWO Vidi Fellowship.

REFERENCES

- Altamirano, D., Patruno, A., Heinke, C., et al. 2010a, The Astronomer's Telegram, 2500, 1
- Altamirano, D., Strohmayer, T. E., Heinke, C. O., et al. 2009, The Astronomer's Telegram, 2182, 1
- Altamirano, D., Patruno, A., Heinke, C. O., et al. 2010b, ApJ, 712, L58
- Bildsten, L. 1998, ApJ, 501, L89
- . 2002, ApJ, 577, L27
- D'Angelo, C. R., & Spruit, H. C. 2012, MNRAS, 420, 416
- Haskell, B., & Patruno, A. 2011, ApJ, 738, L14
- Heinke, C. O., Jonker, P. G., Wijnands, R., Deloye, C. J., & Taam, R. E. 2009, ApJ, 691, 1035
- Heinke, C. O., Altamirano, D., Cohn, H. N., et al. 2010, ApJ, 714, 894
- Kraft, R. P., Mathews, J., & Greenstein, J. L. 1962, ApJ, 136, 312
- Leahy, D. A., Morsink, S. M., & Cadeau, C. 2008, ApJ, 672, 1119
- Mahmoodifar, S., & Strohmayer, T. 2013, ApJ, 773, 140
- Nelson, L. A., & Rappaport, S. 2003, ApJ, 598, 431
- Paczyński, B. 1967, Acta Astron., 17, 287
- Patruno, A., Altamirano, D., & Messenger, C. 2010, MNRAS, 403, 1426
- Patruno, A., Bult, P., Gopakumar, A., et al. 2012, ApJ, 746, L27
- Patruno, A., & D'Angelo, C. 2013, ApJ, 771, 94
- Patruno, A., & Watts, A. L. 2012, in Timing neutron stars: pulsations, oscillations and explosions, ed. T. Belloni, M. Mendez, & C. M. Zhang (in press)
- Patruno, A., Wijnands, R., & van der Klis, M. 2009, ApJ, 698, L60
- Poutanen, J., & Gierliński, M. 2003, MNRAS, 343, 1301
- Psaltis, D., Belloni, T., & van der Klis, M. 1999, ApJ, 520, 262
- Psaltis, D., Özel, F., & Chakrabarty, D. 2014, ApJ, 787, 136
- Rots, A. H., Jahoda, K., & Lyne, A. G. 2004, ApJ, 605, L129
- van Straaten, S., van der Klis, M., & Méndez, M. 2003, ApJ, 596, 1155